Imaging of a spatial distribution of preferred orientation of crystallites by pulsed neutron Bragg edge transmission

Article *in* Journal of Physics Conference Series · December 2010

DOI: 10.1088/1742-6596/251/1/012070

CITATIONS
33

READS
117

5 authors, including:

Hirotaka Sato
Hokkaido University
95 PUBLICATIONS **1,068** CITATIONS

SEE PROFILE

Kenji Iwase
Ibaraki University
89 PUBLICATIONS **872** CITATIONS

SEE PROFILE

Yoshiaki Kiyanagi
Hokkaido University
278 PUBLICATIONS **3,218** CITATIONS

SEE PROFILE

Imaging of a spatial distribution of preferred orientation of crystallites by pulsed neutron Bragg edge transmission

2010 J. Phys.: Conf. Ser. 251 012070

(http://iopscience.iop.org/1742-6596/251/1/012070)

Journal of Physics: Conference Series **251** (2010) 012070 doi:10.1088/1742-6596/251/1/012070

Imaging of a spatial distribution of preferred orientation of crystallites by pulsed neutron Bragg edge transmission

H Sato[1], O Takada[1], K Iwase[2], T Kamiyama[1] and Y Kiyanagi[1]

[1]Graduate School of Engineering, Hokkaido University, Kita-13 Nishi-8, Kita-ku, Sapporo 060-8628, Japan

[2]Frontier Research Center for Applied Atomic Sciences, Ibaraki University, 162-1 Shirakata-shirane, Tokai, Ibaraki 319-1106, Japan

E-mail: hakuryu@eng.hokudai.ac.jp

Abstract. A pulsed neutron transmission coupled with a two-dimensional position sensitive neutron detector gives a time-of-flight spectrum at each pixel of the detector, which depends on the total cross-sections of materials. In order to extract quantitative information of the preferred orientation included in the Bragg scattering total cross-section data, a spectral analysis software for the 2D imaging has been developed, and the transmission data of an unbent iron plate were analyzed. The 2D images with respect to the preferred orientation were successfully obtained, and the effectiveness of spectroscopic neutron transmission imaging was indicated.

1. Introduction

It is very important for improving the strength, the rolling processability and the electromagnetic characteristic depending on the preferred orientation inside a steel sheet to investigate and control the texture. An engineering neutron diffractometer is generally utilized to analyze such crystalline anisotropy inside a material. Moreover, a mapping of such information is performed by the real-space scanning using a pin-point beam, combined with the neutron detectors coupled with a radial collimator.

On the other hand, we have been developing the spectroscopic neutron transmission imaging technique by a time-of-flight (TOF) method at a pulsed source [1], including also energy-selective neutron radiography [2]. For example, there are the spectroscopic Bragg edge radiography for crystallographic imaging [3] and the spectroscopic resonance-absorption tomography for nuclide-selective density imaging and internal thermography [4]. The Bragg edge transmission spectroscopy can give a d-spacing map only with one measurement because it can use a two-dimensional position sensitive neutron detector (2D-PSND) for the imaging of the real-space distribution. This technique has capability to give a 2D real-space distribution of crystal structure information, as requested from material sciences and industrial fields.

So far, the Bragg edge imaging has been applied to a strain imaging [3,5], a crystalline phase imaging [6] and a texture imaging [2,7]. In particular, the quantitative analysis of Bragg edge shapes is indispensable to extract texture information concerning the preferred orientation. Therefore, we present the novel procedure for the imaging of quantitative information of the preferred orientation in a textured material, as well as a Rietveld refinement software development in order to analyze position-dependent pulsed neutron Bragg edge transmission spectra.

2. Experimental

We prepared an experimental sample for which the spatial distribution of the preferred orientation became inhomogeneous due to the plastic deformation. This was a flat iron plate (30 mm height, 105 mm width and 5 mm thickness) stressed at two lines along the height-direction which is parallel to the rolling-direction. This sample was made by bending and unbending at each line. It has been known that this sample has large residual-strain [3], by using the Bragg edge transmission measurement at the spallation neutron source KENS at High Energy Accelerator Research Organization (KEK) in Japan.

The 2D-PSND was the 256 (16×16) pixel ^{6}Li-glass-scintillation detector [8]. The detection efficiency was more than 95 % for cold neutrons. The maximum counting rate was 8.3 MHz/cm^2 which was sufficient for intense beams. The time resolution was set into 10 μs in this experiment. The spatial resolution was 3 mm which was the order of the gauge volume in diffractometry.

The pulsed neutron radiography experiment was carried out at Neutron Beam-line for Observation and Research Use (NOBORU) [9] at Materials and Life Science Experimental Facility (MLF) at Japan Proton Accelerator Research Complex (J-PARC) in Japan. NOBORU directly viewed the decoupled 18 K supercritical para-H_2 moderator at MLF. The MLF accelerator beam power was 4 kW during this experiment. The neutron flight distance from the source to the sample was 14 m. The collimation ratio L / D was 140. The neutron wavelength resolution $\Delta\lambda / \lambda$ at λ = 0.4 nm was 0.35 %.

The unbent iron sample was placed just in front of the 2D imaging detector, and the incident beam and the transmitted beam were measured with the 2D-PSND by using a TOF method simultaneously.

3. Spectral analysis of position-dependent Bragg edge transmission spectra

In order to extract crystallographic information such as preferred orientation from the Bragg edge transmission spectrum obtained at each pixel, we have been developing a new whole-pattern analysis software based on the Rietveld refinement technique [10]. The algorithm was based on the total cross-section simulation code CRIPO [11] and the Bragg edge Rietveld analysis code BETMAn [12].

The neutron transmission spectrum $Tra(\lambda)$ depending on the neutron wavelength λ can be given by

$$Tra(\lambda) = \exp\left[-\sum_{p} \sigma_{tot,p}(\lambda)\rho_p t_p \right]. \quad (1)$$

Here, σ_{tot} is the total cross-section, ρ is the atomic number density and t is the thickness, summed over the number of the crystalline phases p. σ_{tot} of a certain phase consists of elastic coherent, elastic incoherent, inelastic coherent, inelastic incoherent scattering and absorption parts as shown below.

$$\sigma_{tot}(\lambda) = \sigma_{coh}^{ela}(\lambda) + \sigma_{incoh}^{ela}(\lambda) + \sigma_{coh}^{inela}(\lambda) + \sigma_{incoh}^{inela}(\lambda) + \sigma_{abs}(\lambda) \quad (2)$$

The elastic coherent (Bragg) scattering cross-section can be given by

$$\sigma_{coh}^{ela}(\lambda) = \frac{\lambda^2}{2V_0} \sum_{d_{hkl}=0}^{2d_{hkl}<\lambda} |F_{hkl}|^2 d_{hkl} B_{hkl}(\lambda, d_{hkl}) P_{hkl}(\alpha_{hkl}(\lambda)) Ext(\lambda, S). \quad (3)$$

Here, V_0 is the unit cell volume of a crystal. d_{hkl} is the crystal-lattice-plane spacing with respect to the reflection Miller index hkl. The Bragg edge of hkl diffraction appears at $\lambda = 2d_{hkl}$ indicating the back scattering on the Bragg's law. F_{hkl} is the crystal structure factor including the Debye-Waller factor. B_{hkl} is the resolution function describing the Bragg edge broadening [5] due to neutron pulse width. Ext represents the reduction term describing the extinction effect depending on the crystallite size S [13].

P_{hkl} is the probability function of the crystallite orientation depending on α_{hkl} (the acute angle between the incident beam and the orientation of equivalent crystal-lattice-planes $\{hkl\}$) described by

$$\alpha_{hkl}(\lambda) = \frac{\pi}{2} - \arcsin\left(\frac{\lambda}{2d_{hkl}} \right) = \frac{\pi}{2} - \theta_{hkl} \quad (4)$$

where θ_{hkl} is a half of the angle between the incident beam and the diffracted beam. In order to describe the preferred orientation in a Bragg edge transmission spectrum, we used the March-Dollase function [14] as P_{hkl}. This function is used in many Rietveld codes for neutron and X-ray powder diffraction. The March-Dollase function for the transmission geometry [12] is

$$P_{hkl}(\alpha_{hkl}(\lambda)) = \frac{1}{\pi}\int_{-\frac{\pi}{2}}^{\frac{\pi}{2}}\left[\left(r_{hkl}^2 - \frac{1}{r_{hkl}}\right)\left(\cos\alpha_{hkl}(\lambda)\cos\beta_{hkl} - \sin\alpha_{hkl}(\lambda)\sin\beta_{hkl}\sin\phi\right)^2 + \frac{1}{r_{hkl}}\right]^{-\frac{3}{2}} d\phi \quad (5)$$

where r_{hkl} indicates the degree of crystalline anisotropy and β_{hkl} represents the most probable angle of preferred orientation in this study. Since Eq. (5) is described by averaging over φ on the Debye-Scherrer cone, we can investigate orientation information only about θ. r = 1 means the isotropic distribution of crystallites (no preferred orientation). In practice, however, r is not unity because we frequently measure more or less a textured material. The most probable α corresponds to π / 2 - β in case of r > 1, and to β in case of r < 1. These relations are applicable to fiber-shaped crystallites or plate-shaped crystallites. Fig. 1 shows the calculation results of Eq. (2) depending on β_{110} in case of r_{110} > 1, considering only the preferred orientation of {110} crystal-lattice-planes. In this study, we corrected only the longest wavelength Bragg edge shape although a typical Rietveld code considers about the all peaks. This is because it was experimentally examined that the longest wavelength Bragg edge shape can drastically change due to the preferred orientation effect [3], and the correction method of the effect of forward-scattered neutrons detected by 2D detector pixels has not been developed yet. Such forward-scattered neutrons from Fe atoms may increase at $\lambda < 2d_{110}\sin 45°$ (about 0.29 nm).

Next, we tried to extract preferred orientation information β_{110} and r_{110} from the measured pulsed neutron transmission spectra by the Rietveld refinement using a spectral fitting technique. The fitting algorithm was the Levenberg-Marquardt method [15] for a non-linear least-squares estimation. Fig. 2 shows some results of the measured transmission spectra fitted with the Rietveld simulations using Eq. (1). The fitting was improved by introducing the March-Dollase function. Thus, we succeeded in extracting the refined parameters of not only d_{110} but also $\rho \times t$, β_{110} and r_{110}.

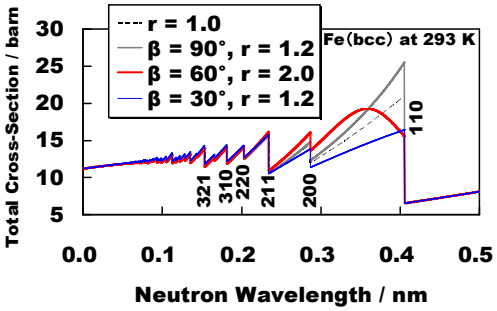

Figure 1. Results of the simulation calculation of the total cross-section depending on the March-Dollase model considering the preferred orientation of a textured polycrystalline material, obtained the developed Rietveld analysis code system for a pulsed neutron Bragg edge transmission spectroscopy.

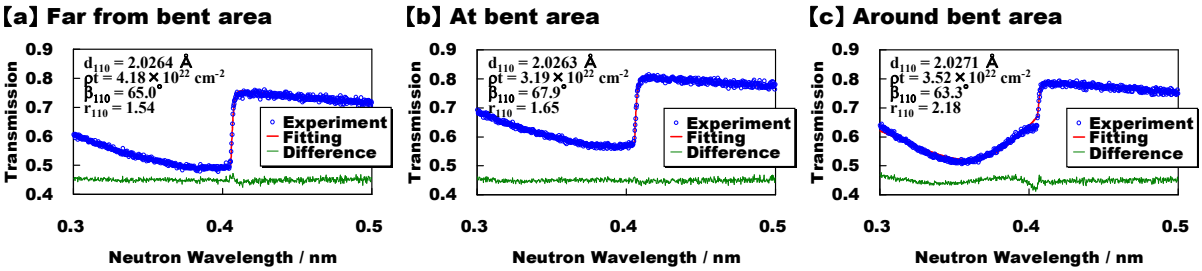

Figure 2. Results of the Rietveld fitting analysis around {110} Bragg edge of the transmission data (a) far from the bent position, (b) at the bent position and (c) around the bent position, measured by the 2D imaging detector. The anisotropic trend becomes strong around the bent area because r is large.

4. Results and discussion

Fig. 3 shows the quantitative images of the projected density of Fe atoms ($\rho \times t$), the most probable angle of the preferred orientation (β_{110}) and the degree of crystalline anisotropy (r_{110}) of the stressed iron sample. Fig. 3 (a) indicates that the density or the thickness decreases only at the bent positions since the $\rho \times t$ values around x = - 13.5 and + 18 mm positions without the plastic deformation are

close to 4.25×10^{22} cm^{-2} (the theoretical value). Fig. 3 (b) indicates that the β_{110} values change to 68° at the bent positions, and to 63° around those. Fig. 3 (c) indicates that the r_{110} values increase above 2.0 only around the bent positions. Thus, the spectroscopic neutron imaging coupled with spectral analyses can non-destructively give the images concerning the physical quantity of a material but not the transmitted neutron intensities. Essentially, these are significant images for crystallography, and are different from the transmission images obtained by an energy-selective neutron radiography.

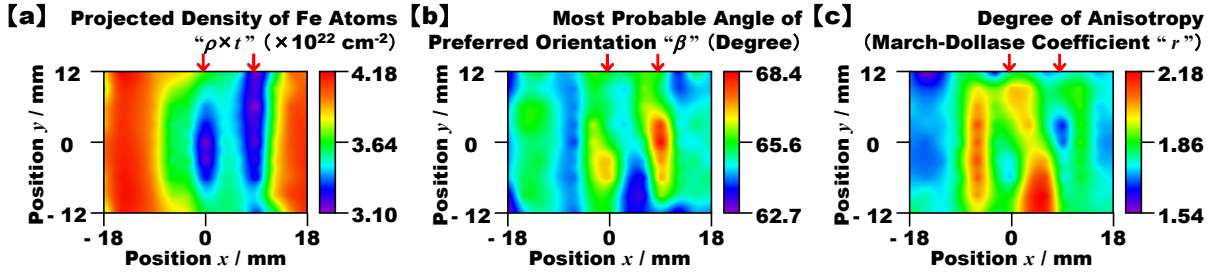

Figure 3. Experimental results of (a) image of the projection data of atomic number density of Fe, (b) image of the most probable angle of preferred orientation and (c) image of the degree of crystalline anisotropy around the stressed area. The allows on the tops of these images indicate the bent lines.

5. Conclusion

We succeeded in taking images of the projected density of atoms, the most probable angle of preferred orientation and the degree of crystalline anisotropy in a textured material simultaneously, using the pulsed neutron Bragg edge transmission method coupled with the Rietveld analysis of position-dependent TOF transmission spectra. These images are useful for crystallography, and this method will become a powerful tool for non-destructive material inspections.

Acknowledgements

The authors are greatly thankful to the NOBORU group [9] and Dr. T. Shinohara of Japan Atomic Energy Agency (JAEA) for experimental assistance at J-PARC. This work was partially supported by Grant-in-Aid for JSPS Fellows (No. 20002121) and Grant-in-Aid for Scientific Research (A) (No. 20246136) from Japan Society for the Promotion of Science.

References

[1] Kiyanagi Y, Kamiyama T, Iwasa H and Hiraga F 2004 *Key Engin. Mater.* **270** 1371
[2] Kockelmann W, Frei G, Lehmann E H, Vontobel P and Santisteban J R 2007 *Nucl. Instr. and Meth. A* **578** 421
[3] Iwase K, Sakuma K, Kamiyama T and Kiyanagi Y 2009 *Nucl. Instr. and Meth. A* **605** 1
[4] Sato H, Kamiyama T and Kiyanagi Y 2009 *Nucl. Instr. and Meth. A* **605** 36
[5] Santisteban J R, Edwards L, Fitzpatrick M E, Steuwer A, Withers P J, Daymond M R, Johnson M W, Rhodes N and Schooneveld E M 2002 *Nucl. Instr. and Meth. A* **481** 765
[6] Steuwer A, Withers P J, Santisteban J R and Edwards L 2005 *J. Appl. Phys.* **97** 074903
[7] Santisteban J R, Edwards L and Stelmukh V 2006 *Physica B* **385** 636
[8] Sato H, Takada O, Satoh S, Kamiyama T and Kiyanagi Y *Nucl. Instr. and Meth. A* (in press)
[9] Maekawa F, Oikawa K, Harada M, Kai T, Meigo S, Kasugai Y, Ooi M, Sakai K, Teshigawara M, Hasegawa S, Ikeda Y and Watanabe N 2009 *Nucl. Instr. and Meth. A* **600** 335
[10] Rietveld H M 1969 *J. Appl. Cryst.* **2** 65
[11] Kropff F and Granada J R 1977 *CAB-1977* Centro Atomico Bariloche, Institute Balseiro
[12] Vogel S 2000 *Ph.D. Thesis* Kiel University
[13] Iwase K, Nagata T, Sakuma K, Takada O, Kamiyama T and Kiyanagi Y 2007 *IEEE Nucl. Sci. Symp. Conf. Rec.* **2** 1716
[14] Dollase W A 1986 *J. Appl. Cryst.* **19** 267
[15] Marquardt D W 1963 *J. Soc. Indust. Appl. Math.* **11** 431